Future Energy
Open Access Journal
ISSN 2832-0328

August 2026| Volume 05 | Issue 03 | Pages 11-24

Journal homepage: https://fupubco.com/fuen

https://doi.org/10.55670/fpll.fuen.5.3.2

Future Publishing LLC

Article

Stochastic energy management strategy for microgrid-connected electric vehicle charging infrastructure

Bhagyashri Govindrao Sherkhane[1,2]*, Sudarshan L. Chavan[3], Aishwrya A. Apted[1]

[1]AISSMS College of Engineering, Pune, India
[2]Zeal College of Engineering and Research, Pune, India
[3]JSPM Rajarshi Shahu College of Engineering, Pune, India

ARTICLE INFO

Article history:
Received 10 January 2026
Received in revised form
28 April 2026
Accepted 04 June 2026

Keywords:
Electric vehicles, Microgrid,
Stochastic optimization, Photovoltaic,
Mixed-integer non-linear programming

*Corresponding author
Email address:
bgsherkhane@gmail.com

DOI: 10.55670/fpll.fuen.5.3.2

ABSTRACT

Ensuring the reliability and stability of standalone microgrids (MGs) is fundamental to the effective integration of renewable energy sources, which are inherently uncertain. This work presents a stochastic optimization model using mixed-integer linear programming (MILP) to determine the optimal operation of electric vehicle charging stations (EVCS) with transactive control, emphasizing the balance between economic efficiency and system reliability. As a result, deploying EVCS will become a vital strategy for integrating renewable energy. An innovative method for supplying electric power from EV fleets involves using transportation networks as additional infrastructure. This article proposes that transportation networks, EVCS, and MGs can be optimally scheduled under uncertain photovoltaic (PV) generation using transactive control. The stochastic optimization problem is formulated as a mixed-integer nonlinear program and implemented in a moving-horizon framework for real-time onboard operation. The framework is tested on the IEEE 30-bus transmission network. The results show the efficiency of the proposed framework as an improvement tool for economic performance and operational stability in renewable-integrated power markets, and it reduces peak loads through the coordinated charging and discharging of vehicles.

1. Introduction

1.1 Motivation

In today's era, the renewable energy sources (RES) industry has gained significance as the world transitions to cleaner power sources away from fossil fuels [1]. In 2014, the global renewable generation capacity was 1829 GW; by 2022, it had increased by 84.36% to reach 3372 GW, according to the International Renewable Energy Agency (IRENA) [2]. The addition of renewable sources such as solar and wind PV systems has enabled local generation, storage, and load management [3]. The uncertain and variable nature of RES challenges the safe and cost-effective operation of power networks. Modern power systems are evolving due to road transportation and the growth of solar and wind resources. Microgrids (MGs), which stay connected to the utility grid, provide a valuable platform for integrating variable loads, storage systems, and local renewable energy sources. Electric vehicles (EVs) form a significant portion of variable loads; while their charging introduces uncertainty, it also creates opportunities for transactive management and two-way energy exchange [4,5]. Battery electric vehicles (BEVs) rely on onboard batteries for propulsion [6]. In contrast, plug-in hybrid electric vehicles (PHEVs) combine an internal combustion engine with a battery-powered drive system, enabling them to draw power from both traditional fuel and electricity [7]. An EV system with transactive control can balance supply and demand by incorporating transactive control into a stochastic framework alongside other parameters. When integrated with transactive system management, the proposed strategy should consider the roles of EV charging stations (EVCS), MG, and RES. Effective scheduling in these systems must, however, take into account mobility-driven demand, electricity price volatility, and uncertainty in renewable output. Although deterministic formulations are computationally efficient, they often yield suboptimal schedules because they do not account for sources of variability. On the other hand, stochastic models use probabilistic data, which enables operators to plan for a variety of potential operating scenarios. Aspects of this issue have been studied independently in the past, with an

emphasis on EV integration, price variability, or renewable uncertainty. There are very few attempts to integrate these elements into a single framework, and there remains a dearth of empirical testing of common distribution standards. The current work fills this gap by developing and evaluating a stochastic problem for a grid-connected MG that includes battery storage, EVCS with transactive control, and solar photovoltaic (PV) and wind generation.

1.2 Literature review

Driven by the worldwide need to reduce carbon emissions, curb reliance on fossil fuels, and address environmental degradation, electric vehicles (EVs) have become a dominant technology in the transportation sector. However, a significant obstacle to the widespread adoption of EVs remains the lack of an effective, widely dispersed charging infrastructure. When applied to situations with high uncertainty in consumer load and RES, these models frequently produced unrealistic schedules despite their computational simplicity. Stochastic and scenario-based formulations have been widely used to overcome these constraints [8,9]. To reflect the variability of renewable resources and energy market prices, these approaches generate multiple realizations of uncertain variables. The computational load is then controlled while preserving the statistical characteristics of the original dataset using scenario reduction techniques. Results in this field consistently show that stochastic programming outperforms deterministic scheduling in predicted operating costs and dependability. The integration of EVCS into grid-connected MG operations is another crucial research area. Because they serve as mobile loads and, when vehicle-to-grid (V2G) operation is enabled, can also act as distributed storage, EVs offer flexibility [10–12]. Coordinated charging lowers peak demand, boosts the use of renewable energy sources, and promotes cost-effectiveness, according to studies. Nevertheless, most research focuses solely on EVs, ignoring market pricing dynamics or renewable variability.

Modern power networks can be made more reliable and operationally efficient with battery storage devices. In times of high availability, they enable the absorption of excess energy from renewable sources such as solar and wind and the release of stored energy when demand outpaces supply [13]. By doing this, they reduce dependence on greenhouse gas emissions, promote increased renewable penetration, and stabilize the grid. The long-term relevance of battery storage for sustainable energy has been further reinforced by ongoing technological advancements that have enabled higher capacities and more affordable options [14]. Battery storage offers significant flexibility in managing EV charging needs. This feature supports the broader shift toward low-carbon, sustainable transportation by improving the integration of wind and solar PV into EVCS and preserving voltage stability [15]. The best locations for fast-charging stations and their effects on the distribution network have been the subject of numerous studies. To reduce power loss, EV charging stations were integrated into the road and electrical networks [16]. Fast-charging station location, in conjunction with renewable energy integration, has been investigated [17], with renewable-based charging stations examined to improve voltage stability and cost-effectiveness. Particle swarm optimization has been used to study fast-charging station location while taking into account the traffic flow [18] model; nevertheless, transactive control expansion scheduling of EVCS has not been addressed. The coordinated dispatching of EVCS within the transportation network using transactive control has not been overlooked by the aforementioned studies.

Optimal EV placement and its effects on the transmission network have been the subject of several studies [19,20]. To reduce power losses, EV charging stations were integrated into a road-and-electrical network. Fast-charging station locations in conjunction with renewable energy integration have been investigated [21], with renewable-based charging stations examined to improve voltage stability and cost-effectiveness. Reference [22] developed a stochastic model for transactive control that included energy storage, plug-in hybrid electric vehicles, renewable resources, and fuel cell-based heat and thermal units. A mixed-integer nonlinear program (MINLP) was used to model the context, including hydrogen storage for the fuel cell units. The modified honey badger algorithm was used to optimize intelligent charging schemes. To enhance transactive control in the context of solar PV and EVCS, reference [23] proposed a hybrid approach that combines particle swarm optimization with quantum self-attention neural networks. Reference [24] explored the efficiency, viability, and environmental advantages of integrating EVs and renewable energy in deregulated electricity systems. Their research focused on the impact of renewable energy on emissions and on energy storage, smart charging, and demand response, which might enhance power flow and system security. The study examined methods to enhance power flow regulation and system decentralization and concluded that hybrid renewable systems might reach grid parity under favorable pricing conditions.

Most studies on the EVCS model have already been detailed; additional studies have employed stochastic approaches to determine the optimal scheduling time for EVCS in the energy transportation network [25]. The techno-economic feasibility of various facilities, including transportable energy storage, railway lines, and conveying roads, is assessed using a stochastic problem [26]. Coordinated planning of transportation networks and electric power systems improves grid stability, eases traffic congestion, and strengthens the integration of renewable energy and electric vehicles [27]. To lower overall operating costs, reduce traffic congestion, and enhance wind energy integration, the implications of EVCSs in coupled traffic-electric networks are investigated [28]. The stochastic problem in electric traffic networks with thermal units and the challenges of the transportation traffic model are solved. The transportation network, however, received little attention in the literature [29]. A transportable EVCS is incorporated into a two-stage stochastic model to manage PV uncertainty and enable transmission system flexibility [30]. Additionally, variable EV charging methods would improve the efficiency of transportation infrastructure and MG operations. More focus is being placed on integrating EVs with transactive energy management and on the growing deployment of energy resources such as solar panels and energy storage devices. A dynamic pricing system is used by

an EVCS located inside office buildings with rooftop PVs to set transactive control rates for energy exchange between EVs [31]. The best scheduling of privately owned EVCSs is integrated into a transactive market structure between EVCSs and a remote PV farm using a predefined power purchase market [32]. A market-based network of EV charging stations that employs transactive energy management is described in Reference [33]. Previous research has used a variety of methods to investigate EVCS investment costs under transactive control and DC network security from various angles. While addressing the optimal problem of EVCS via fleets in power networks, none of the studies in the literature examined the interplay among grid-connected MG operations, uncertain solar PV output, and electricity pricing.

1.3 Research gaps and paper contribution

Although existing studies have extensively explored wind-solar configuration with EV scheduling optimization from the perspectives of resource complementarity, security stability, and uncertainty, several key challenges remain for practical operation in high-penetration renewable energy systems. First, most studies focus on single objectives such as curtailment rate, output fluctuation, construction cost, or energy storage scale, while neglecting the significant coupling and trade-offs among these objectives in high-penetration systems, vehicle charging, and market price volatility in MG [10,11]. Second, although attention has been paid to wind-solar complementarity, the coordinated consideration of load profiles, transmission characteristics, and demand-response constraints remains insufficient, and a unified, multi-parameter analytical framework integrating source, EVCS, and grid factors has yet to be established. Several studies consider both renewable and non-renewable generating units. However, flexible sources such as demand response, solar PV, and EVCS should be integrated into the power system to enhance network operation and security.

To the best of the authors' knowledge, references [26–28, 31–33] are the only studies that have simultaneously addressed transactive energy management in EV transportation networks. Table 1 summarizes recent work. To bridge the knowledge gap between accurate physical modeling and computational efficiency, this study proposes a stochastic optimization day-ahead dispatching of the power system with EVCS, considering operational flexibility. The first stage relies on forecasts of renewable energy output, power load demand, electricity procurement from the main grid, and the output of generating power units. The second stage integrates wind-solar output characteristics, market price characteristics, and load characteristics into a production MG model and evaluates different wind-solar ratio schemes across four dimensions: scenario generation and reduction, curtailment rate, EVCS scale, and system cost. Ultimately, a comprehensive optimal ratio balancing technical and economic performance is derived. A mixed-integer linear programming (MILP) algorithm is presented to solve the proposed stochastic day-ahead dispatching model, in which integer variables are incorporated in the second stage. The main contributions of this paper are outlined as follows:

1) Introduces a stochastic scheduling approach for optimizing the integration of RESs and EVCS into transmission networks, improving performance, reducing curtailment, enhancing reliability, and minimizing costs within an MG operation.

2) Addresses the stochastic behavior of RESs, effectively integrating uncertain energy sources into transmission networks, such as market price and load characteristics.

3) In order to reduce traffic congestion and enhance power grid economics, a transactive control is implemented to streamline energy exchanges between transportation networks for EVCS throughout interconnected MGs. Focuses on maximizing techno-economic performance by enhancing system flexibility and efficiently integrating the transportation network with a grid-connected MG.

Table 1. Comparison of the main features of the conventional and proposed work

Ref no.	EVCS	MG	DCOPF	Transactive control	RES uncertainty		Proposed model
					Wind	Solar PV	
[8]	✓	✓	-	-	-	-	• Cooperative optimization • Single-objective
[10]	✓		-	-	✓	-	• Non-Cooperative optimization • Single-objective
[16]	✓	-	✓	-	✓	-	• Non-Cooperative optimization • Single-objective
[21]	✓	-	✓	✓	✓	-	• Cooperative optimization • Single-objective
[22]	✓	✓	-	-	✓	✓	• Cooperative optimization • Single-objective
[26]	✓	-	✓	-	✓	-	• Non-Cooperative optimization • Single-objective
[28]	✓	-	✓	-	✓	-	• Cooperative optimization • Single-objective
[31]	✓	-	✓	-	-	✓	• Cooperative optimization • Single-objective
[33]	✓	-	✓	✓	✓	-	• Non-Cooperative optimization • Single-objective
This paper	✓	✓	✓	✓	✓	✓	• Two- stage stochastic optimization • Single objective

1.4 Organization

The remainder of this paper is organized as follows. Section 2 presents the system configuration and describes the proposed stochastic formulation. Section 3 presents scenario generation and reduction techniques. Section 4 presents the problem formulation: objectives, constraints, and the GAMS-based solver. Section 5 presents the solution methodology. Section 6 validates the effectiveness of the proposed method through case studies using IEEE 30-bus data. Finally, Section 7 concludes the paper.

2. Distribution characteristics of solar PV and wind resources

2.1 Modeling of PV

MG incorporates solar PV generation, a clean, emissions-free energy source, as part of its sustainable energy supply. Because PV output depends on environmental factors, it is inherently variable despite its benefits. Definitions of each parameter are given in constraints (1) and (2), which give the problem formulation of solar PV generation [22].

$$P_h^{pv} = P_{STC,h}^{pv} \cdot \frac{I_{cell}^{rad}}{1000}\left(1 + \beta(T^c - 25)\right) \quad (1)$$

Signifies the cut-out speed, and W_i indicates the cut-in speed.

$$T^c = T^a + \left(\frac{I_{cell}^{rad}}{800}\right)(T^n - 20) \quad (2)$$

In these equations, P_h^{pv} denotes the output power of the solar PV units in watts (W), although $P_{STC,h}^{pv}$ links to the rated output below standard test conditions.

2.2 Modeling of WT

Wind speed uncertainty using the Weibull distribution can be expressed as follows [19]: Constraint (3), output power of the wind turbine P_h^{wt} is modeled as a role of the wind speed S_h^{wt}. The parameters S_{CIN}^{wt} and S_{CO}^{wt} represent the cut-in and cut-out speeds, respectively. The cut-in speed is the minimum wind velocity at which the turbine begins producing power; below this threshold, no energy is generated. The wind speed S_R^{wt} at which the turbine reaches its rated output power is indicated by the rated speed P_R^{wt}.The turbine is now producing its maximum safe power output while operating at maximum efficiency [12].

$$P_h^{wt} = \begin{cases} 0 S_h^{wt} < S_{CIN}^{wt} \\ P_{r,h}^{wt}\left(\frac{(S_h^{wt})^3 - (S_{CIN}^{wt})^3}{(S_R^{wt})^3 - (S_{CIN}^{wt})^3}\right) S_{CIN}^{wt} < S_h^{wt} < S_R^{wt} \\ P_R^{wt} S_R^{wt} < S_h^{wt} < S_{CO}^{wt} \\ 0 S_h^{wt} \geq S_{CO}^{wt} \end{cases} \quad (3)$$

3. Uncertainty characterization

3.1 Generation of scenarios

This work employs a hybrid approach combining Gaussian copulas, Latin Hypercube Sampling with Dependence (LHSD), and Affinity propagation (AP), as shown in Figure 1. Copulas model dependencies among random variables by linking their marginal distributions. LHSD combined with copulas generates representative scenario sets that accurately capture inter-temporal RE dependencies, after which Affinity Propagation clustering selects the final subset. Independent Latin Hypercube Sampling points are first generated in standard normal space N(μ,σ). These samples are then transformed via the inverse cumulative distribution function to match the specified marginal distributions. Inter-variable dependence is introduced by applying the Cholesky decomposition to the covariance matrix, producing correlated multivariate normal samples. These correlated samples are subsequently converted to their uniform counterparts U (0,1) using the cumulative distribution function. Finally, the uniform samples are mapped through the inverse marginal distributions of the fitted univariate models, yielding scenarios that preserve both the original marginal distribution and the inter-temporal dependence structure. Since large scenario sets can render stochastic programming intractable, Affinity Propagation clustering, an exemplar-based method that exchanges messages between data points to identify representative clusters, is applied after LHSD to reduce computational complexity while preserving representative diversity. To capture the range of possible outcomes more effectively, each PDF is separated into some intervals. An example of a PDF partitioned into seven intervals is illustrated in Figure 1 [18]. Furthermore, to generate a diverse set of scenarios with assigned probabilities, a roulette-wheel selection mechanism is used, as depicted in Figure 2.

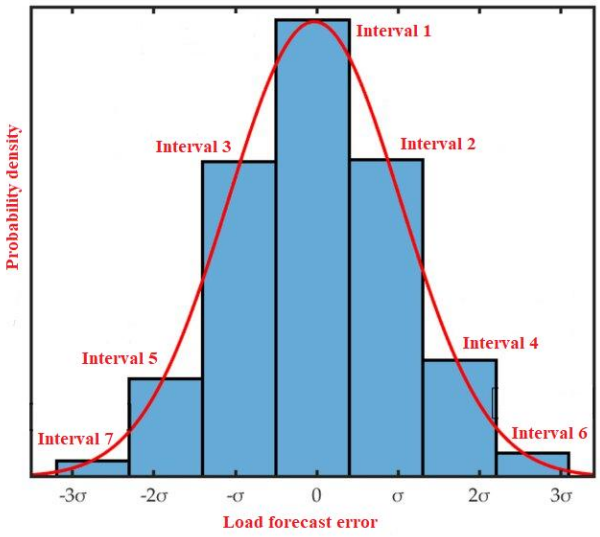

Figure 1. Simple MCS fits the normal distribution

Figure 2. Normal Distribution fit by the Weibull method

3.2 Scenario reduction

The computational overhead that results from modeling uncertainty with a large number of scenarios may be too great. The fast-forward scenario-reduction approach is used in this work to address this problem [18,19]. The following summarizes the algorithm's primary steps:

Step 1: Calculate the separation among every pair of possibilities with constraint (4).

$$-f(\tau,\tau^{-}) = \sum_{i\in PV,WT}|P^{\tau} - P^{\tau-}| \quad (4)$$

Step 2: Determine the mean separation between every scenario and every other scenario. The first scenario to be chosen is the one with the lowest average distance.

$$\tau_1 = arg\left\{\min_{\tau^{-}\in\Lambda}\sum_{\tau\in\Lambda}\pi_{\tau}\upsilon(\tau,\tau^{-})\right. \quad (5)$$

$$\Lambda_S = \Lambda_S U\{\tau_1\} \quad (6)$$

$$\Lambda_j = \Lambda_j U\{\tau_1\} \quad (7)$$

Step 3: Calculate the distance between each unselected scenario and each previously chosen scenario. After selecting the scenario that minimizes this distance, both the non-selected and selected sets are updated.

$$\tau_i = arg\left\{\min_{\tau^{-}\in\Lambda_j}\sum_{\tau\in\Lambda_j\setminus\{\tau^{-}\}}\pi_{\tau}\min_{\tau--\in\Lambda_s U\{\tau\}}\upsilon(\tau,\tau^{--})\right. \quad (8)$$

$$\Lambda_S = \Lambda_S U\{\tau_i\} \quad (9)$$

$$\Lambda_j = \Lambda_j U\{\tau_i\} \quad (10)$$

Step 4: The probability of every unselected scenario is transferred to the nearest chosen scenario. Here, $j(\tau)$ denotes the non-selected situation that is most likely to be the selected situation τ.

$$\pi_{\tau}^{*} = \pi_{\tau} + \sum_{\tau^{-}\in j(\tau)}\pi_{\tau^{-}} \quad (11)$$

$$\tau = arg\left\{\min_{\tau--\in\Lambda_S}\upsilon(\tau^{--},\tau^{-})\right. \quad (12)$$

4. Problem formulation

The microgrid interacts with the main grid based on the output of generation units and the consumption of electrical loads. The objective of the system is to minimize the combined costs of economic and security indicators through an optimal power system. Adhering to the principle of prioritizing renewable energy sources, operating according to the dataset output, regardless of operating costs.

4.1 Formulation of cost function

The objective function (O.F.) formulation in this paper incorporates base-scenario dispatch with scenario-based adjustments [15,16], reflecting real-world market operations. Therefore, the real-time power balancing cost comprises the adjustment cost of the thermal power unit's output, EV charging costs, and the overall cost of the microgrid, which includes the battery storage cost (BSSC). This proposed optimization problem accounts for correlations among random input factors, such as solar PV and wind, to determine the optimal dispatch, power ratings, and charging/discharging schedules for each EV fleet, ensuring proper system operation. The complete mathematical formulation of this objective function is provided in constraint (13).

$$\begin{aligned} min \quad & \sum_{t\in T}\sum_{s\in S}\pi_s\left(\sum_{j\in ncg}C(P_{cg_{j,s,t}}) + \right. \\ & \left.\sum_{i,j\in pv}\beta_{i,h}^{pv}.C^{pv}P_{i,s,t}^{pv} + \sum_{i,j\in wt}\gamma_{i,t}^{wt}.C^{wt}P_{i,s,t}^{wt} + \sum_{i\in e}BSSC_{s,e,t}\right) \\ & + \left(\sum_{s\in S}\pi_s\left(\sum_{ev\in E}I_{ev_s}^{V2G}THC_{ev}^{fd,V2G}\left(\sum_{t\in T}\sum_{ev\in E}\left(IT_{ev_{n,s,t}}TH_{ev_{n,s,t}}\right) + \right.\right.\right. \\ & \left.\left.\left.\left(CF_{ev}^{dc,V2G}P_{ev_{s,t}}^{dch}\right)I_{ev_{s,t}}^{dch}\right)\right)\right) \end{aligned} \quad (13)$$

The costs for RES units per hour h are signified by C^{pv} and C^{wt}, respectively. The total cost of the BSSC comprises several elements, including the initial capital investment and the replacement costs incurred over the system's operational lifetime. The capital investment cost, ICC_{BS} , is directly linked to the capacity for power $P_{BS,s}^{c}$ and the capacity for energy $E_{BS,s}^{c}$ of the storage system and is clear in constraint (5).

$$ICC_{BS} = \left(P^{cost}.P_{BS,s}^{c}\right) + \left(E^{cost}.E_{BS,s}^{c}\right) \quad (14)$$

Where, P^{cost} and E^{cost} represent the cost coefficients corresponding to the storage system's power and energy capacities, respectively.

$$N_{BS}^{cy} = \sum_{i=1}^{24} count_{BS}(h,t) \quad (15)$$

$$Count_{BS}(h,t) = (S_h - S_{h-1})S_h, \forall h \in 24 \quad (16)$$

$$BS_{REP} = \frac{PD}{BS_{LFC}} \quad (17)$$

$$BSSC = \frac{1}{24.PD}\left(\frac{i(1+i)^{PD}}{(1+i)^{PD}-1}.ICC_{BS}.BS_{REP}\right) \quad (18)$$

The first step in determining how many replacements are needed over the course of the project is to determine how many charge and discharge cycles occur per year. signified as N_{BS}^{cy}. Constraints (15) and (16), where (16) is definite $Count_{BS}(h,t)$, the cycle count for hour h on working day t is used to compute this value. Therefore, the total number of replacements, BS_{REP}, the project lifetime is stated by constraint (17). Lastly, the day-to-day price of the storage, signified as BSSC, is designed in constraint (18) by including the primary capital cost $ICC_{BS}$and the appropriate interest rate (i).

4.2 EVCS constraints

These constraints are based on the likely values of uncertainty parameters and include constraints and equations for the network, thermal units, RESs, MG, and EV fleets. Although EV fleets operate on hourly schedules, the system can be complex because they are connected to the grid at both work and home. EV fleets are represented by binary variables, as shown in equations (19)- (20), which indicate whether they are at work, at home, or on the road. The connected links of a specific commuter route can be used to model the energy levels and toll-free continuous states described in constraints (21-31). These links mimic the energy and toll-free states shown in constraints (21) and (22). Additionally, the grid acts as a storage system for the EV fleet, representing V2G input. EV fleets also have defined minimum and maximum energy capacities. Therefore, the various transportation constraints include:

$$\sum_{t\in HtoW}IT_{ev_{n,s,t}} \geq TR_{ev_t}, \forall s, \forall ev, \forall n \quad (19)$$

$$\sum_{t\in WtoP}IT_{ev_{n,s,t}} \geq TR_{ev_t} \forall s, \forall ev, \forall n \quad (20)$$

$$FE_{ev_{n,s,t}} = \sum_{m\in M} \zeta_{ev_{m,s,t}} CE_{ev_{m,t}} \forall s, \forall ev, \forall n \quad (21)$$

$$TH_{ev_{n,s,t}} = \sum_{m\in M} \zeta_{ev_{m,s,t}} CT_{ev_{m,t}} \forall s, \forall ev, \forall n \quad (22)$$

$$IH_{ev_{n,s,t}} + IW_{ev_{n,s,t}} + IT_{ev_{n,s,t}} = 1, \forall s, \forall n, \forall ev, \forall t \quad (23)$$

$$I^{dch}_{ev_{s,t}} + I^{ch}_{ev_{s,t}} \le IH_{ev_{n,s,t}} + IW_{ev_{n,s,t}}, \quad \forall s, \forall ev, \forall n \quad (24)$$

$$I^{dch}_{ev_{s,t}} \le I^{V2G}_{ev_s}, \forall s, \forall ev, \forall t \quad (25)$$

$$\sum_{n\in TS_e} I_{ev_{n,s}} = 1, \forall ev, \forall s \quad (26)$$

$$P^{\min}_{ev} \sum_{n\in TS_e} I_{ev_{n,s}} IH_{ev_{n,s,t}} \le P^{HO}_{ev_{s,t}} \le P^{\max}_{ev} \sum_{n\in TS_e} I_{ev_{n,s}} IH_{ev_{n,s,t}}, \forall s, \forall ev, \forall t \quad (27)$$

$$P^{\min}_{ev} \sum_{n\in TS_e} I_{ev_{n,s}} IW_{ev_{n,s,t}} \le P^{WP}_{ev_{s,t}} \le P^{\max}_{ev} \sum_{n\in TS_e} I_{ev_{n,s}} IW_{ev_{n,s,t}}, \forall s, \forall ev, \forall t \quad (28)$$

$$P^{HO}_{ev_{s,t}} + P^{WP}_{ev_{s,t}} = P^{ch}_{ev_{s,t}} - P^{dch}_{ev_{s,t}}, \forall s, \forall ev, \forall t \quad (29)$$

$$I^{ch}_{ev_{s,t}} + I^{dch}_{ev_{s,t}} \le \sum_{n\in TS_{ev,t}} I_{ev_{n,s}} \left(IH_{ev_{n,s,t}} + IW_{ev_{n,s,t}}\right), \forall s, \forall ev, \forall t \quad (30)$$

$$CE^{\min}_{ev} \le CE_{ev_{s,t}} \le CE^{\max}_{ev}, \forall s, \forall ev, \forall t \quad (31)$$

Constraint (23) models the EV fleet as a single state at each hour; Constraint (24) indicates that the EV fleet contributes to the grid by sharing electricity from homes or workplaces; and Constraint (25) indicates that the supply of EV fleet power to the grid occurs while engaged in charging mode. The EV fleet's trip plan state, or binary status, is represented by constraint (26). The inequality constraints on the exchange of power between the grid and the EV fleet are given by constraints (27)-(28), which account for charging/discharging rates and the fleet's current conditions. The electricity exchange among the house, office, and the grid, similar to charging and discharging in each solar PV scenario, is represented by constraint (29). According to the travel plan, constraint (30) describes the EV fleet's charging/discharging conditions, which can occur only while parked. Constraints (32) and (33) specify the primary and final energy necessities, while constraint (20) defines the maximum/minimum capacity of EV fleets. Constraint (34) provides the battery's state of charge (SOC), which is the sum of the SOC during transport, charging, and discharging modes. Constraint (35) shows the battery energy balance. Constraints (36) and (37) use a linear function of charging and discharging power to approximate the SOC. The initial energy value of each EV fleet, the charging/discharging capacity, and the SOC must all be recalculated continuously at specific stages of the procedure.

$$CE_{ev_{s,0}} = CE_{ev_0} \quad \forall s, \forall ev, \forall t \quad (32)$$

$$CE_{ev_{s,T}} = CE_{ev_T} \quad \forall s, \forall ev, \forall t \quad (33)$$

$$CE_{ev_{s,t+1}} = CE_{ev_{s,t}} + SOC_{ev_{s,t}} \quad \forall s, \forall ev, \forall t \quad (34)$$

$$SOC_{ev_{s,t}} = SOC^{ch}_{ev_{s,t}} - SOC^{dch}_{ev_{s,t}} - SOC^{T}_{ev_{s,t}}, \forall s, \forall ev, \forall t \quad (35)$$

$$0 \le P^{dch}_{ev_{s,t}} \le P^{\max}_{ev} I^{dch}_{ev_{s,t}}, \forall s, \forall ev, \forall t \quad (36)$$

$$0 \le P^{ch}_{ev_{s,t}} \le P^{\max}_{ev} I^{ch}_{ev_{s,t}}, \forall s, \forall ev, \forall t \quad (37)$$

4.3 Power balance and transmission constraints

Each unit's power generation should be maintained between the minimum and maximum limits of active and reactive power, as shown in Equations (38) and (39). The sum of the powers generated by the thermal, renewable, and EV fleets, during charging/discharging, should equal the load demand in each sample scenario, as specified by equation (40). Equations (41) and (42) show the DC security and network line flow limits for renewable power samples, respectively. The following are the subject technical constraints for each period in every sample:

$$P^{\min}_{cg_j} \le P_{cg_{j,s,t}} \le P^{\max}_{cg_j}, \forall s, \forall t \quad (38)$$

$$Q^{\min}_{cg_j} \le Q_{cg_{j,s,t}} \le Q^{\max}_{cg_j}, \forall s, \forall t \quad (39)$$

$$\sum_{j\in ncg} P_{cg_{j,s,t}} + \sum_{i\in pv} \beta^{pv}_{i,h} P^{pv}_{i,s,h} + \sum_{i\in wt} \gamma^{wt}_{i,h} P^{wt}_{i,s,h} + \sum_{i\in Bus} \sum_{ev\in E} \left(P^{dch}_{ev_{s,t}} - P^{ch}_{ev_{s,t}}\right) = \sum_{i\in nl} PD_{i_t} + \sum_{i,j\in Bus} P_{loss} \quad \forall s, \forall t \quad (40)$$

$$-P^{\min}_{i,j} \le P_{i,j,s,t} \le P^{\max}_{i,j}, \quad \forall t, \forall s \quad (41)$$

$$P_{i,j,s,t} = \frac{\phi_{s,i,t} - \phi_{s,j,t}}{z_{i,j}}, \forall t, \forall s \quad (42)$$

4.4 RES power output constraints

Both photovoltaic (PV) and wind turbine (WT) devices have output power limited by their respective minimum/maximum generation capacities, as shown in constraints (43) and (44).

$$P^{pv}_{\min} \le P^{pv}_{i,s,t} \le P^{pv}_{\max} \quad (43)$$

$$P^{wt}_{\min} \le P^{wt}_{i,s,t} \le P^{wt}_{\max} \quad (44)$$

This section outlines the scenario-based framework for capturing uncertainties in electrical demand (ED), wind generation, and PV output.

5. Solution algorithm

A two-stage stochastic scheduling problem is formulated to address the objective function (constraint 13), using a CPLEX solver [34] and an optimization approach to handle the stochastic problem with EVs and MG. The proposed model determines the charging and discharging performance of each EV fleet using the starting grid data, as described in constraints (29) and (30). Based on market power pricing and battery capacity, all EV fleets are routed to the closest arrival time. Parking lots are given the EV scheduling challenge only when the requirements are satisfied. Lastly, every EV fleet has a 24-hour transactive-control MG with optimal generation dispatch. Constraints (29) and (30) describe how to determine the charging and discharging performance of each EV fleet using the initial grid data, as suggested in the stochastic model. Based on market power pricing and battery capacity, all EV fleets are guided to the closest arrival time. Parking lots are the only places where the EV scheduling problem is assigned if the requirements are satisfied. Lastly, each fleet of EVs has a grid-connected MG with optimal generation dispatch based on transactive control over a full day. To improve day-ahead EV fleet dispatch and minimize operating costs while respecting system constraints, this

study employs a two-stage stochastic scheduling approach that incorporates RES power. As illustrated in Figure 3, it introduces energy transporters and uses a transactive management-based solution for MG, renewable energy, and EV fleets.

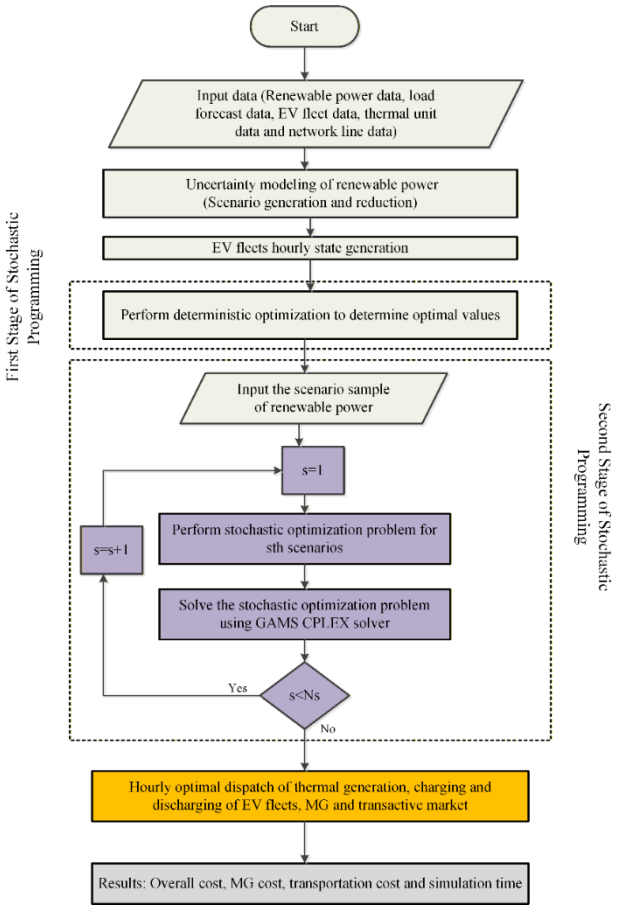

Figure 3. Proposed algorithms

6. Case Study

To evaluate the effectiveness of the proposed EV optimization strategy in transmission networks, a renewable energy–integrated model with grid-connected microgrids is tested. Network scheduling scenarios based on transactive control are analyzed in this section. The proposed stochastic optimization model, considering wind and solar PV generation, is simulated using the CPLEX solver and GAMS on a modified IEEE 30-bus test system.

6.1 Parameter setting and data description

The modified IEEE 30-bus system is taken from reference [35] and includes nine thermal units, two solar PV farms (RES), and 41 network lines. The generator's maximum load is 386 MW, while its total installed capacity is 470 MW. Figure 4 displays the hourly load, wind, and solar PV profiles. Assume that the network line connects two cities, orange and green, as depicted in Figure 5. Also, two solar PV farms with a combined capacity of 75 MW at bus 23 (green city) and 100 MW at bus 1 (orange city). Figure 6 shows the EV fleets and traffic network structures for each city. Also, the hourly energy prices are \$18, \$28, and \$35. The presence of wind and solar resources with a total capacity of 100 MW requires effective scheduling strategies to optimize energy generation and storage.

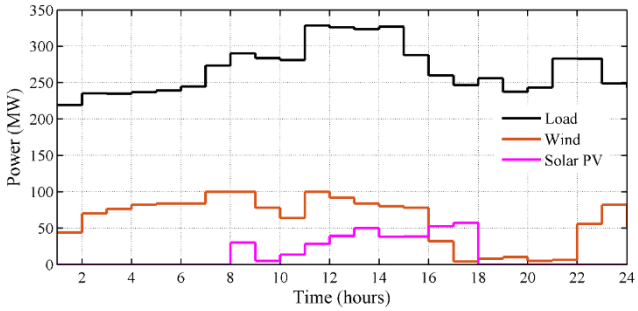

Figure 4. Hourly load, wind, and solar PV profile

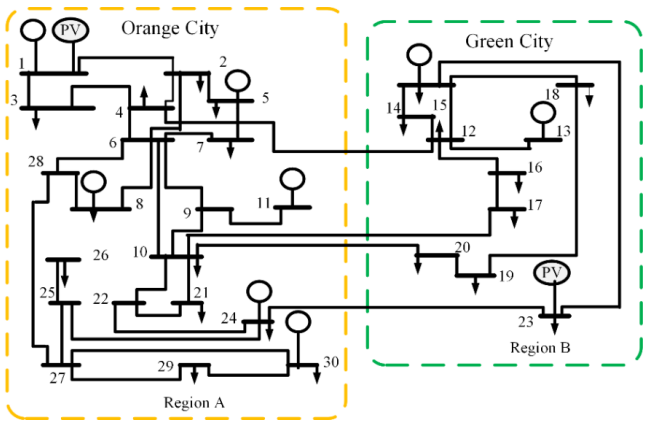

Figure 5. Network power in the IEEE 30-bus system

According to expected traffic patterns, 4,500 EVs will be divided over four fleets. It displays several EV fleets from two cities; for instance, OF1-OF4 show four different EV fleets from Orange and Green. Table 2 also displays the maximum and minimum capacities of each city fleet, as well as the maximum exchange power of each fleet. It then displays the network home node and the related bus of the EV fleet, followed by the workplace network and the consistent bus of the EV fleet. The mapping between the traffic network and power grid buses is shown in Table 3. The minimum capacity is set at 30% of the battery capacity, and the battery cost is fixed at \$30 per car per year and \$20 per MWh [32]. It is assumed that the driving energy required to travel one way is the same as that required to return to the starting point.

Based on expected traffic patterns, five fleets of 50,000 EVs will be allocated [35]. In these buses, the network parameter 30,000 EVs are distributed across nodes 1, 3, 7, 21, and 23, with counts of 12,000, 10,000, 8,000, 14,000, and 6,000, respectively. With a typical charging/discharging power of 248/210.8 kW, the network operator analysis zone can accommodate up to 50,000 EVs in the schedule. The fleet and travel characteristics of electric vehicles are described in Reference [36]. One-way travel requires as much energy as returning to the starting point.

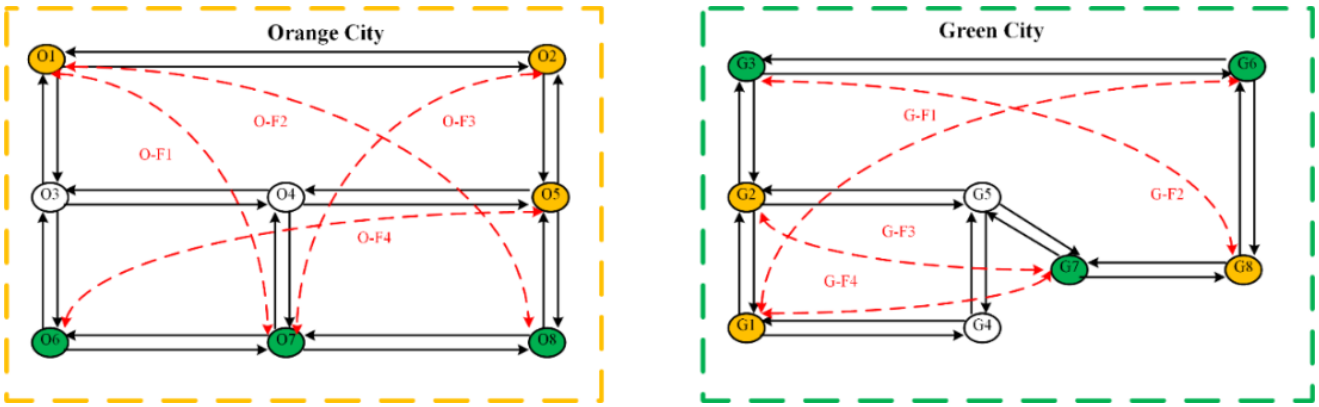

Figure 6. EV traffic network in the IEEE 30-bus system

Table 2. Information on EV fleets in the IEEE 30-bus system

EV Fleets	Number of EV	Home node	Work node	Min. Cap. (MWh)	Max. Cap. (MWh)	Max. Power Exc. (MW)
O-F1	1500	1 (O1)	8 (O7)	32	180	26
O-F2	1000	1 (O1)	11 (O8)	22	120	16
O-F3	1000	5 (O2)	21 (O7)	22	120	16
O-F4	1000	7 (O5)	30 (O6)	22	120	16
G-F1	1500	14 (G4)	17 (G6)	32	180	26
G-F2	1000	18 (G3)	20 (G8)	22	120	16
G-F3	1000	15 (G2)	23 (G7)	22	120	16
G-F4	1000	13 (G1)	23 (G7)	22	120	16

Table 3. Planning of the EV transportation system data in the IEEE 30-bus system

Blue City	Node No.	Green City	Node No.
O1	1	G1	13
O2	5	G2	15
O3	9	G3	18
O4	28	G4	14
O5	7	G5	12
O6	30	G6	17
O7	21	G7	23
O8	11	G8	20

6.2 Modeling of uncertainty

Initially, 1,000 scenarios were created to illustrate uncertainty in load and RES output using historical data. In scenario-based optimization models, the computational complexity and solution time are directly influenced by the number of scenarios considered. While generating a large number of scenarios is necessary to capture the full range of doubts in the system, handling them simultaneously can be computationally prohibitive, especially for large-scale applications. Therefore, a scenario-reduction process is essential to make the optimization tractable without significantly compromising the quality of the results. Choosing a smaller subset of situations while maintaining the key statistical and probabilistic features of the original full set is the main objective of scenario reduction.

The fast-forward selection technique was used to reduce this enormous set to a representative set of 10 scenarios, thereby reducing the computational load. Figures 7 to 9, which show the hourly fluctuations of load, solar PV power output, and WT power production, respectively, illustrate the clustering of these reduced scenarios.

6.3 Simulation results

To demonstrate the effectiveness of the two-stage stochastic dispatching model, this case study is performed on an IEEE 30-bus system. A system is used to implement the proposed strategy and evaluate the impact of optimizing EV fleets with a grid-connected MG on system operation. The following three cases are used in this section to examine the flexibility of resources:

1) Case 1: Deterministic with thermal and renewable power.
2) Case 2: Stochastic with EV fleets and renewable power.
3) Case 3: Stochastic with EV fleets, renewable, and grid-connected MG.

Case 1: This section evaluates the impact of integrating generating units and renewable power on system operating costs. Figure 10 shows that coordinating the schedules of generating units with renewable power optimizes energy use, reducing overall energy consumption. Thermal units G1, G2, G5, and G9 are dispatched for the entire 24-hour period. This saved energy will be used in the upcoming hours when the system load is high. When demand increases, the stored energy will be consumed accordingly. Since Bus 1 has the most affordable renewable power and grid units, the system is designed to draw the majority of its electricity from it.

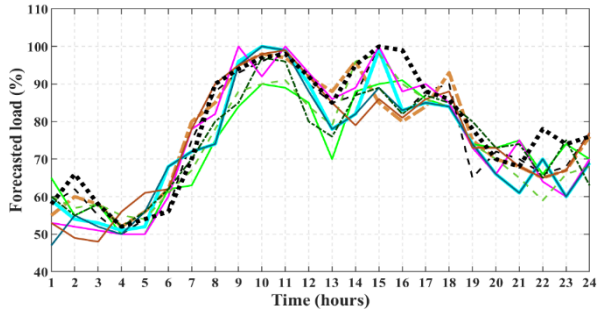

Figure 7. Hourly load scenarios clustered within the MG

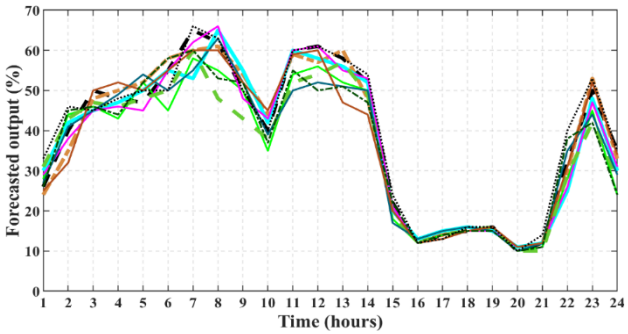

Figure 8. Hourly wind output power scenario clustering

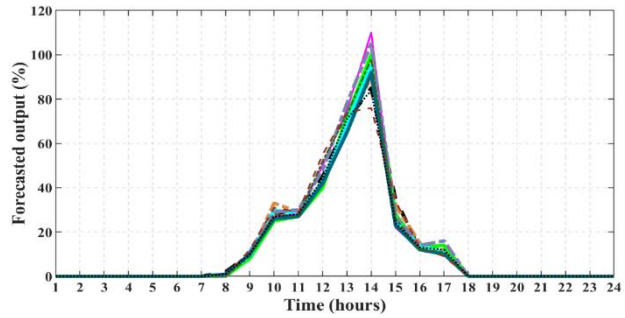

Figure 9. Hourly PV output power scenario clustering

However, as shown in Figure 11, units G3, G6, and G7 are scheduled between 4–12 hours, while units G4 and G8 are scheduled from 13–24 hours. As a result, the system has not fully utilized the grid operation provided by heat unit 1 and RES power. Units G7 and G8 will therefore be dispatched between 12 and 22 hours. With an RES farm, the total system operation cost is $221,322.76, which is less than the $235,524.77 cost without RES electricity.

Case 2: The thermal and electric vehicle transportation in stochastic problems with renewable power is shown in Fig. 11. The benefits of establishing 100% EV fleets are explained in this case study. For 24 hours, the initial units G1, G5, and G9 are always scheduled. Units G2, G4, and G6 are scheduled between 6 and 24 hours, although units G7 and G8 are scheduled between 21 and 24 hours. EV fleets may change the network energy load profile, as illustrated in Figure 11. Between 16 and 17, when EV traffic is concentrated on Bus 4 and lines 1-4 are congested, demand peaks. Bus 1 is therefore unable to schedule to meet the load professionally during this time. Bus 1 is therefore unable to dispatch efficiently to meet demand at this time. Furthermore, G3 is unable to schedule well due to the magnitude of the network lines. Compared to Case 1, which used renewable electricity, the total cost in this instance is $218,762.37, $2,560.39 lower.

The hourly loss curve of the MG with and without BS is shown in Figure 12. Between hours 15 and 21, when demand is at its highest, system losses increase dramatically in the absence of BS. This pattern illustrates the inefficiencies that arise when high loads must be supplied only by the grid. However, the loss profile becomes more dynamic with BS integration. Losses marginally rise while the batteries are charging during times of low demand because more grid power is consumed. During peak hours, this tendency reverses as stored energy is released, relieving grid stress and lowering losses. These findings demonstrate that BS not only increases the MG's resilience but also boosts operational effectiveness by reducing losses during periods of high demand.

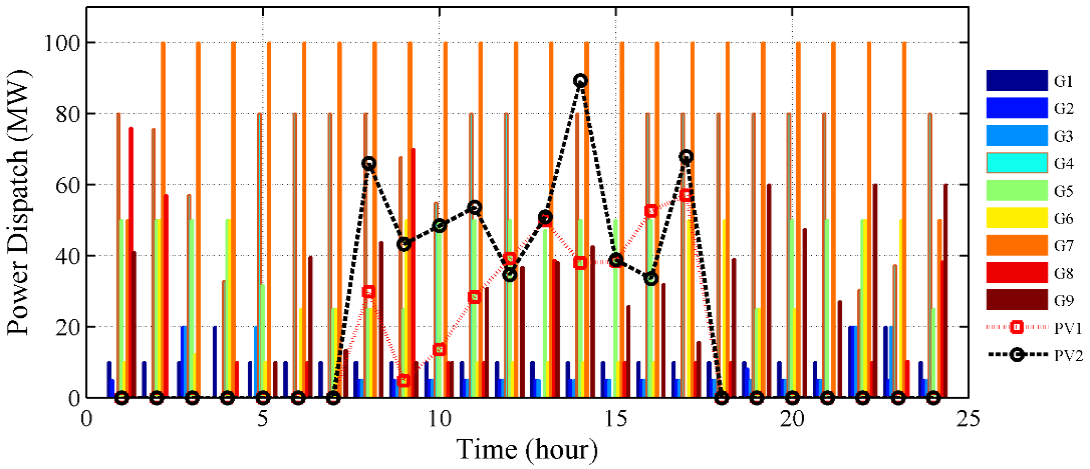

Figure 10. Dispatch of the generating unit with renewable power

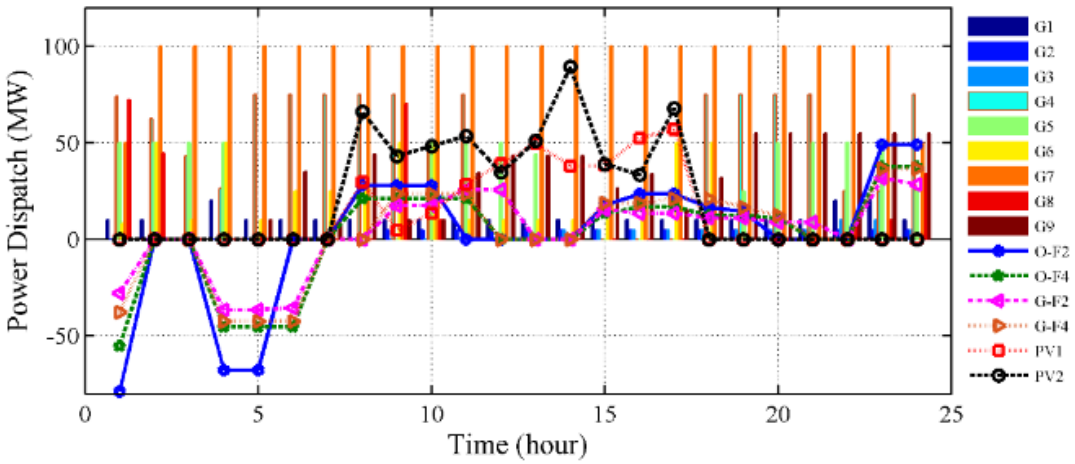

Figure 11. Dispatch of generating units with EV fleets and renewable power

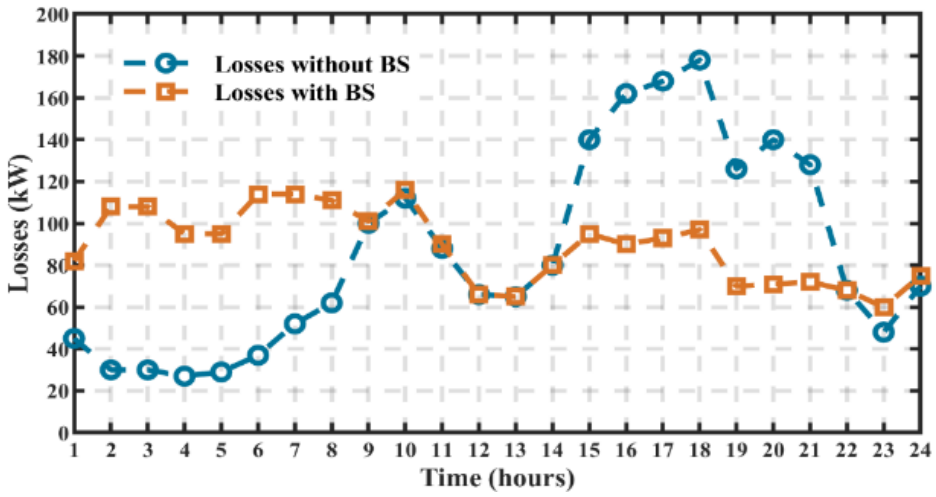

Figure 12. Hourly losses in Case 2 with and without storage integration

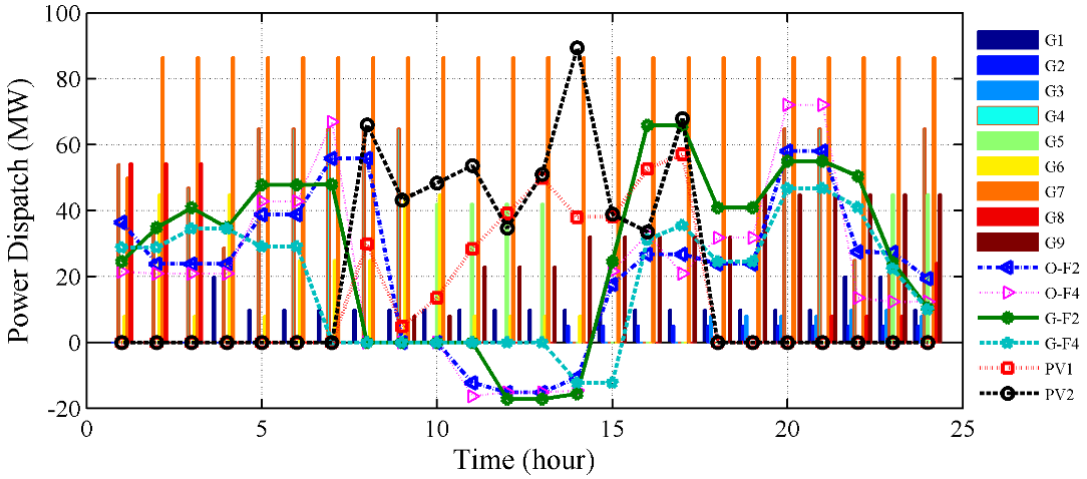

Figure 13. Dispatch of generating units with EV fleets and grid-connected MG

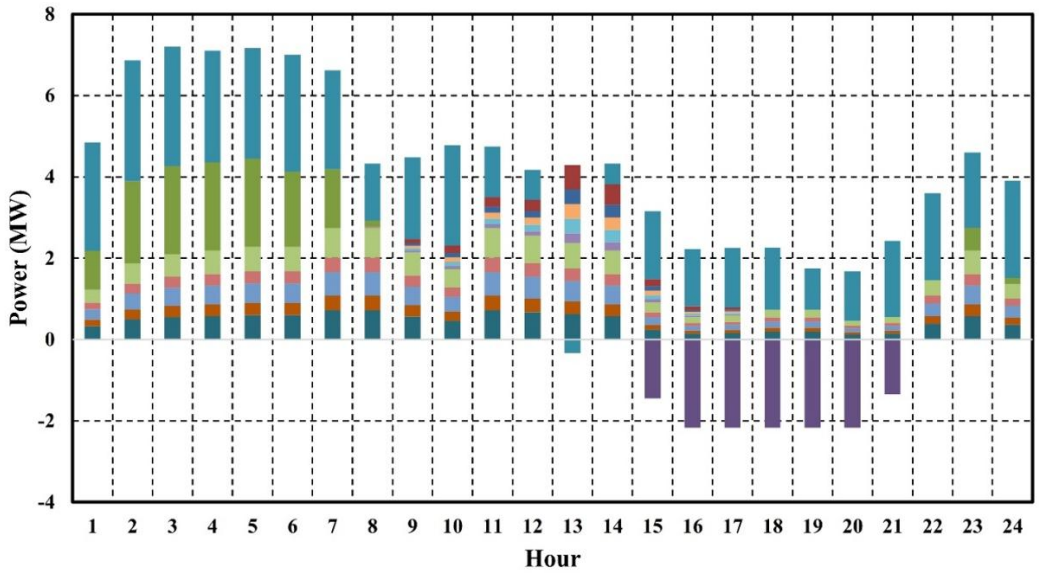

Figure 14. The main grid's economic schedule

Case 3: This study integrates EV fleets, renewable power scenarios, and transactive control within a scheduling framework using stochastic optimization. Uncertainty in renewable power is managed through the fast-forward methodology and stochastic optimization techniques. The dispatch process for Case 3, involving a grid-connected MG, is illustrated in Figure 13. Each EV fleet can ultimately achieve a uniform load distribution by significantly lowering the peak value and increasing the minor valleys. By including the storage charging and discharging cycles, Figure 14 expands on this analysis. Because extra renewable power is captured during low-demand hours and stored energy can be used during high-cost or peak-demand periods, the addition of BS further increases the efficiency of energy distribution. In addition to increasing the use of renewable energy, this coordinated scheduling reduces dependence on the main grid, lowers overall costs, and boosts system resilience.

6.4 Economic analysis

Table 4 illustrates the dispatch cost results for three cases. Since Case 1 ignores uncertainty, it has the lowest thermal cost. However, Case 2 examines the performance of EV users' systems during the intra-day economic dispatch stage, from when they left their houses at 6 a.m. to when they returned at 5 p.m. Compared with Case 3, the operational costs for EV fleets are higher, at $217,533.61 and $189,300.89 for traffic assignment. The reason for this disparity is that the stochastic solution for Case 1 lacks robustness, preventing it from guaranteeing safe and dependable system operation in real time. The improved performance of the energy market is consistent with these outcomes.

Table 4. Cost comparison of three cases

Cases	Operating costs ($)	Thermal costs ($)	Traffic costs ($)	BS costs ($)	CPU time (s)
1	221322.76	221322.76	--	--	554
2	218762.37	217533.61	1228.76	--	897
3	206543.35	189300.89	887.65	16354.81	1130

The overall cost and simulation time for every case are described in Table 4. Three different sorts of EV consumers are also assumed in this scenario: 1) Early Party: leaves home at 6 a.m. and arrives back at 4.30 p.m. early; 2) Normal Party: leaves home at 7 a.m. and arrives back at 5 p.m. Early party EV fleets are O-F1, O-F2, G-F1, and G-F2, while standard party EV fleets are O-F3, O-F4, G-F3, and G-F4. In the first case, the total cost of the renewable units is $ 221,322.76. Without including EV fleets and the MG, the base-case thermal costs are $ 221,322.76. When EVs are used, the total system cost is reduced by approximately $ 2,560.39. Case 3 has the lowest traffic cost, whereas Case 2 has the highest, owing to increased network congestion from EV fleets and renewable scenarios. The study evaluates how EVCS enhances system flexibility under different EV penetration levels. EV fleet size and RES capacity scale up proportionally, while thermal power plant parameters remain unchanged.

7. Conclusion

In this research, the transactive management condition was employed to thoroughly analyze renewable power generation and its impact on the EV fleet and the grid-connected MG. This would ensure financial benefits for system operators, EV fleets, and MG for participating in the transmission network. The constraints were reserve, transmission, EVCS, thermal operation, and network constraints. However, by successfully minimizing load-shedding events and reducing operating expenses, the suggested approach demonstrates improved economic performance during real intra-day operations. The system would be an MINLP, but such problems have local optima and are computationally expensive. The analogous MILP model was developed to quickly obtain a globally optimal solution with minimal error. Uncertain parameters, such as the quantities of EVs and renewables, were included in the model. As a result, the normal probability density function was used to characterize pertinent scenarios. The fast-forward scenario reduction technique was then used to extract high-probability scenarios. When considering the grid-connected MG and BS, the suggested methods may be cost-effective and

efficient for power markets and load management. The findings demonstrate that the proposed method outperforms the stochastic method. Overall, provides valuable insights into optimizing renewable-powered EV charging stations, enhancing their reliability and sustainability. Further research should focus on advancing loss allocation methodologies, leveraging AI-driven demand forecasting, integrating battery energy storage systems, and developing policy-driven incentives to optimize EV infrastructure deployment. Moreover, advanced scenario reduction techniques and learning–based uncertainty forecasting may be employed to further improve computational efficiency and capture emerging dynamics in high-renewable, high-EV MGs.

Ethical issue

The authors are aware of and comply with best practices in publication ethics, specifically concerning authorship (avoidance of guest authorship), dual submission, manipulation of figures, competing interests, and compliance with policies on research ethics. The authors adhere to publication requirements that the submitted work is original and has not been published elsewhere in any language.

Data availability statement

The manuscript contains all the data. However, more data will be available upon request from the corresponding author.

Conflict of interest

The authors declare no potential conflict of interest.

References

[1] Bourek, Yacine, Chouaib Ammari, Ayyoub Zouaghi, and Loris Pace. "Optimization and decision-making approach for energy storage strategies in a natural gas processing facility with photovoltaic renewable energy supply." Journal of Energy Storage, vol. 112, 2025, 115431.

[2] https://www.irena.org/.

[3] Nguyen, Thuan Thanh, Thang Trung Nguyen, and Hoai Phong Nguyen. "Optimal operation of battery energy storage system in microgrid to minimize electricity cost based on model predictive control using coyote algorithm." Journal of Energy Storage, vol. 114, 2025, 115904.

[4] Acedo Aguilar, J., & Wang, S. (2025). Impacts of electric vehicles on traffic-power systems: A review. International Journal of Sustainable Transportation, 19(2), 103–120.

[5] Moralejo Piñas, J., Martinez-Gil, F., Soriano Santacruz, M., & Fernández, F. (2025). Electric vehicle market dynamics: A multi-agent approach to policy, infrastructure, and consumer behavior. Energy Policy, 206, 114800.

[6] Song, J. (2025). Evaluation of driving resistance and energy consumption in electric vehicles under various ambient and tire temperatures using real-world driving data. ETransportation, 25, 100454.

[7] Qin, J., Huang, H., Lu, H., & Li, Z. (2025). Energy management strategy for hybrid electric vehicles based on deep reinforcement learning with consideration of electric drive system thermal characteristics. Energy Conversion and Management, 332, 119697.

[8] Hai, T., Alazzawi, A. K., Mohamad Zain, J., & Oikawa, H. (2023). A stochastic optimal scheduling of distributed energy resources with electric vehicles based on a microgrid considering electricity price. Sustainable Energy Technologies and Assessments, 55.

[9] Albarakati, A. J., Boujoudar, Y., Azeroual, M., Eliysaouy, L., Kotb, H., Aljarbouh, A., Khalid Alkahtani, H., Mostafa, S. M., Tassaddiq, A., & Pupkov, A. (2022). Microgrid energy management and monitoring systems: A comprehensive review. Frontiers in Energy Research, 10.

[10] Zakaria, A., Duan, C., & Djokic, S. Z. (2024). Hosting capacity of distribution networks for controlled and uncontrolled residential EV charging with static and dynamic thermal ratings of network components. IET Generation, Transmission and Distribution, 18(6).

[11] Muttaqi, K. M., Isac, E., Mandal, A., Sutanto, D., & Akter, S. (2024). Fast and random charging of electric vehicles and its impacts: State-of-the-art technologies and case studies. Electric Power Systems Research, 226.

[12] Alrubaie, A. J., Salem, M., Yahya, K., Mohamed, M., & Kamarol, M. (2023). A Comprehensive Review of Electric Vehicle Charging Stations with Solar Photovoltaic System Considering Market, Technical Requirements, Network Implications, and Future Challenges. In Sustainability (Switzerland) (Vol. 15, Issue 10).

[13] Rezvani, Alireza, Majid Gandomkar, Maziar Izadbakhsh, and Abdollah Ahmadi. "Environmental/economic scheduling of a micro-grid with renewable energy resources." Journal of Cleaner Production 87 (2015): 216-226.

[14] Izadbakhsh, Maziar, Majid Gandomkar, Alireza Rezvani, and Abdollah Ahmadi. "Short-term resource scheduling of a renewable energy-based micro grid." Renewable energy 75 (2015): 598-606.

[15] Bukar, Abba Lawan, Chee Wei Tan, and Kwan Yiew Lau. "Optimal sizing of an autonomous photovoltaic/wind/battery/diesel generator microgrid using grasshopper optimization algorithm." Solar Energy 188 (2019): 685-696.

[16] Gallo M, Marrasso E, Martone C, Pallotta G, Roselli C, Sasso M. (2025). Energy, economic, and environmental benefits of a car-sharing system with electric vehicles integrated into a renewable-energy community. Sustain Energy Technol Assessments 81:104428.

[17] Sayarshad, H. R. (2025). Integrating renewable energy and electric vehicle participation into regulation markets to enhance grid stability. Energy Conversion and Management, 342, 120041.

[18] Sahoo, J. P., Sivasubramani, S., & Srikar, P. S. S. (2025). Optimized framework for strategic electric vehicle charging station placement and scheduling in distribution systems with renewable energy integration. Swarm and Evolutionary Computation, 95, 101943.

[19] Y. Wang, and J. S. Thompson, “Two-stage admission and scheduling mechanism for electric vehicle

charging," IEEE Transactions on Smart Grid, vol. 10, no. 3, pp. 2650-2660, 2019.
[20] C. Luo, Y. F. Huang, and V. Gupta, "Stochastic dynamic pricing for EV charging stations with renewable integration and energy storage," IEEE Transactions on Smart Grid, vol. 9, no. 2, pp. 1494-1505, 2018.
[21] J. Yang, T. Wiedmann, F. Luo, G. Yan, F. Wen, and G. H. Broadbent, "A fully decentralized hierarchical transactive energy framework for charging EVs with local DERs in power distribution systems," IEEE Transactions on Transportation Electrification, pp. 1-1, 2022.
[22] Ju, Y., Wang, S., Ren, J., Wang, L., & Abdalla, A. N. (2025). Advanced scheduling of energy storage, renewable generation, and hydrogen management in microgrids with plug-in hybrid electric vehicle charging integration. International Journal of Hydrogen Energy, 136, 609–624.
[23] Manikandan, M., Saravanan, R., Kannayeram, G., & Saravanan, M. (2025). Integrating renewable resources and electric Vehicles: An approach for effective energy management in DC microgrid. Solar Energy, 299, 113775.
[24] Das, S. S., Vadlamudi, B., Vital, M. L. N., Dawn, S., Rao, K. D., Cali, U., & Ustun, T. S. (2025). A comparative analysis of the efficient coordination of renewable energy and electric vehicles in a deregulated smart power system. Energy Reports, 13, 3136–3164.
[25] Li K, Shao C, Zhang H, Wang X. "Strategic Pricing of Electric Vehicle Charging Service Providers in Coupled Power Transportation Network". IEEE Trans Smart Grid. 14(3):2189-201, 2023.
[26] Sun, Y., Chen, Z., Li, Z., Tian, W., and Shahidehpour, M., "EV charging schedule in coupled constrained networks of transportation and power system", IEEE Trans. on Smart Grid, Vol. 10, No. 5, pp. 4706-4716, August 2018.
[27] Gan W, Shahidehpour M, Yan M, et al. "Coordinated planning of transportation and electric power networks with the proliferation of electric vehicles". IEEE Trans Smart Grid. 2020; vol: 11, p. 4005- 4016. Sept.2020.
[28] Qian T, Li X, Wang X, Shahidehpour M. "Enhanced coordination of electric power and transportation networks via EV charging services". IEEE Trans Smart Grid. 2020; vol. 3, p. 1271-1279. July 2020.
[29] L. Affolabi, M. Shahidehpour, W. Gan, M. Yan, B. Chen, S. Pandey, A. Vukojevic, E. A. Paaso, A. Alabdulwahab, and A. Abusorrah, "Optimal transactive energy trading of electric vehicle charging stations with on-site PV generation in constrained power distribution networks," IEEE Transactions on Smart Grid, vol. 13, no. 2, pp. 1427-1440, 2022
[30] N. Liu, Q. F. Chen, X. Y. Lu, J. Liu, and J. H. Zhang, "A Charging Strategy for PV Based Battery Switch Stations Considering Service Availability and Self-Consumption of PV Energy," IEEE Trans Ind Electron, vol. 62, no. 8, pp. 4878-4889, Aug 2015.
[31] S. Aznavi, P. Fajri, M. B. Shadmand, and A. Khoshkbar-Sadigh, "Peer-to-peer operation strategy of PV equipped office buildings and charging stations considering electric vehicle energy pricing," IEEE Transactions on Industry Applications, vol. 56, no. 5, pp. 5848-5857, 2020.
[32] N. A. El-Taweel, H. Farag, M. F. Shaaban, and M. E. AlSharidah, "Optimization model for EV charging stations with PV farm transactive energy," IEEE Trans. on Industrial Informatics, vol. 18, no. 7, pp. 4608-4621, 2022.
[33] L. Affolabi, M. Shahidehpour, W. Gan, M. Yan, B. Chen, S. Pandey, A. Vukojevic, E. A. Paaso, A. Alabdulwahab, and A. Abusorrah, "Optimal transactive energy trading of electric vehicle charging stations with on-site PV Generation in constrained power distribution networks," IEEE Transactions on Smart Grid, vol. 13, no. 2, pp. 1427-1440, 2022.
[34] Generalized Algebraic Modeling Systems (GAMS). [Online]. Available: http://www.gams.com.
[35] Gupta PP, V.N. Kalkhambkar, Sharma CK , Jain P, and Bhakar R. "Optimal electric vehicles charging scheduling for energy and reserve markets considering wind uncertainty and generator contingency" International Journal of Energy Research, Vol. 46, no. 4, pp: 4516-4539, 2022.
[36] Todakar, K. M., Gupta, P. P., Kalkhambkar, V., & Sharma, K. C. (2024). Optimal scheduling of battery energy storage train and renewable power generation. Electrical Engineering, 106(5), 6477-6493.

List of symbols

Variables	
$CE_{ev_{s,t}}$	Energy capacity of EV fleets *ev*
$P_{cg_{j,s,t}}, Q_{cg_{j,s,t}}$	Active and reactive power of generation at the unit *cg*
$PSH_{d,t}$	Shiftable load at time *t* in the base case
$DeR_{d,t}^{up}, DeR_{d,t}^{dn}$	Scheduled load up and down time at times *t*
$FE_{ev_{n,s,t}}, TH_{ev_{n,s,t}}$	EV fleet unit *ev* of toll-free and energy-efficient travel plans
$CE_{ev_{s,0}}, CE_{ev_{s,T}}$	Initial/terminal energy storage capacity of the unit EV*ev*
$SR_{cg_{j,s,t}}, SR_{ev_{s,t}}$	Spinning reserve of generation and EV fleet unit cg and *ev*
$P_{ev_{s,t}}^{dch}, P_{ev_{s,t}}^{ch}$	Discharging/charging power of the EV fleet unit *ev*
$IH_{ev_{n,s,t}}, IW_{ev_{n,s,t}}$	Binary variable for home and workplace states of the EV fleet unit *ev*
$IT_{ev_{n,s,t}}$	Binary variable for the travelling states of the EV fleet unit *ev*
$I_{ev_{s,t}}^{dch}, I_{ev_{s,t}}^{ch}$	Status of charging and discharging of the EV fleet unit *ev*
$I_{ev_{n,s}}, I_{ev_s}^{V2G}$	Status of travel plan and V2G program of the EV fleet unit *ev*
$r_{cg_{j,s,t}}^{up}, r_{cg_{j,s,t}}^{dn}$	Up and down regulation of generation at the unit *cg*
$P_{ev_{s,t}}^{HO}, P_{ev_{s,t}}^{WP}$	Discharging/charging the power of the workplace and home of the unit EV fleet*ev*
$SOC_{ev_{s,t}}, SOC_{ev_{s,T}}$	Initial/final increment of unit EV fleet *ev*
$SOC_{ev_{s,t}}^{dch}, SOC_{ev_{s,t}}^{ch}$	Discharging/charging the power of the SOC of the unit EV fleet *ev*
Indices and Sets	
d, D	Index and set of demand block
t, T	Index and set of time in hours
j, ncg	Index and set of the thermal unit
s, S	Index and set of scenario samples
n	Indices of EV fleet *ev* travel
m, M	Index of EV fleet *ev* traffic network connected link
ev, E	Index and set of EV fleets
i, j	Index of network buses
Parameters	
TR_{ev_t}	EV fleet *ev* travel time *t*
$CF_{ev}^{dc,V2G}$	EV fleet *ev* degradation cost with the V2G program
$MADeR_{d,t}$	Maximum adjustable load
$PFD_{d,t}$	Forecasted demand power at the time *t*
$THC_{ev}^{fd,V2G}$	EV fleet *ev* fixed degradation cost with the V2G program
$RE_{cg_t}^{up,max_{cg_t}^{dn,max}}$	Regulation up and down at the unit *cg*
$CE_{ev}^{min_{ev}^{max}}$	Mini/ max energy capacity of EV fleet *ev*
$CE_{ev_{m,t}}, CT_{ev_{m,t}}$	EV fleet *ev* of energy and toll-free traffic network in time *t*
CE_{ev_0}, CE_{ev_T}	Initial/terminal stored energy capacity of the unit EV fleet *ev*
$P_{ev}^{min_{ev}^{max}}$	Mini/max power of the unit EV fleet *ev*
π_s	Probability of solar PV scenario samples *S*
PD_{i_t}, SR_t	Total demand and spinning reserve in time *t*
$Q_{cg}^{max_{cg}^{min}}$	Max/min of reactive power generating unit cg
$P_{cg}^{max_{cg}^{min}}$	Max/min of active power generating unit cg
Z_{ij}	Impedance of the bus i to j
$P_{i,j}^{max_{i,j}^{min}}$	Max/min network line of bus i to j